COMMUNICATION

ChemComm
www.rsc.org/chemcomm

Characterisation of pillared clays by contrast-matching small-angle neutron scattering

Th. A. Steriotis,*[a] K. L. Stefanopoulos,[a] U. Keiderling,[b] A. De Stefanis[c] and A. A. G. Tomlinson[c]

[a] *NCSR 'DEMOKRITOS', Institute of Physical Chemistry, Aghia Paraskevi Attikis, 153 10 Athens, Greece. E-mail: tster@chem.demokritos.gr; Fax: +30 010 6511766; Tel: +30 010 6503973*

[b] *Hahn Meitner Institut, BENSC, Glienicker Strasse 100, D-14109 Berlin, Germany. E-mail: keiderling@hmi.de; Fax: +49 030 80693059; Tel: +49 030 80692339*

[c] *Istituto per lo Studio dei Materiali Nanostrutturati, Area della Ricerca di Roma del CNR, C.P.10, 00016 Monterotondo Staz, (RM), Italy. E-mail: gus@mlib.cnr.it; Fax: +39 06 90672322; Tel: +39 06 90672322*

Received (in Cambridge, UK) 29th July 2002, Accepted 30th August 2002
First published as an Advance Article on the web 19th September 2002

The contrast-matching SANS technique has been utilised to determine inter-pillar distances (and surface texture) in montmorillonite and beidellite pillared smectite clays; they lie in the range 1.40–1.80 nm, reflecting different inter-pillar orderings.

Interest in pillared inter-layered clays (PILCs) has over the past decade been centred on their prospective industrial utilisation in catalysis (de-NOx), sorption and separations (air–gas mixtures, small hydrocarbons, multi-component hydrocarbon mixtures, large organic molecules).[1] The materials (which have a highly heterogeneous structure because they contain both nano-oxide pillars cross linked to aluminosilicate clay layers) are produced after intercalating large inorganic cations between smectite clay layers but their unique micro/meso pore system does not allow application of single crystal X-ray techniques.[2] However, their pore network structure is being unravelled with the aid of non-conventional micropore characterisation techniques[3] as well as X-ray absorption spectroscopy.[2,4] On the other hand, Small-Angle Neutron Scattering (SANS) is an excellent technique for characterising porous materials on a scale covering a range from 1 nm to >200 nm.[5] The scattered intensity depends on the contrast in the neutron scattering length density of the different phases in the sample. The neutron scattering length density, ρ, of a molecule of i atoms can be readily calculated by the expression:

$$\rho = \sum_i b_i \frac{dN_A}{M_w} \quad (1)$$

where b_i is the scattering length of the individual atoms in the molecule, d is the bulk density of the scattering object, M_w is its molecular weight and N_A is the Avogadro number. Neutrons have the advantage over X-rays that their scattering length varies completely irregularly with the atomic number, even with isotopes of the same element. The fact that hydrogen and deuterium have scattering lengths of opposite sign means that, unlike X-rays, neutrons can not only 'see' hydrogen isotopes but they can also differentiate between them. It is then possible to match the scattering density of one phase in a multiphase material with an appropriate mixture of H_2O–D_2O. As a result, contrast matching is achieved and the structural characterisation of the unmatched phases is feasible.[6]

We have employed contrast-matching small-angle neutron scattering (SANS) to independently resolve the structure of each phase in alumina-pillared and Mg/alumina-pillared samples. Using this technique, pores are filled with appropriate ratios of H_2O–D_2O that match the neutron scattering length density of each phase (clay, pillars) such that scattering from samples with filled pores results only from the non-contrast matched phase.

The PILCs studied were: the parent clay, EFW (Extra Fine White) a montmorillonite kindly provided by IKO-Erbslöh (Germany) and B4, a Greek beidellite provided by Silver & Baryte Ores Mining CO. SA. Additionally, pillared Al_2O_3 EFW (Al-EFW) and Mg/Al oxide pillared EFW (MgAl-EFW) as well as Al_2O_3 pillared B4 (Al-B4) and its Fe/Al oxide pillared analogue (FA-B4) were used. The Al_2O_3 PILCs were prepared as reported previously[7] and MgAl-EFW (a new material) by the usual procedure of adding an aqueous solution of poly-hydroxyoxyaluminium Keggin ion (15 meq Al and 1 meq Mg per g clay) to a colloidal dispersion of EFW. The intercalated precursor was allowed to flocculate, decanted, dialysed to remove Cl^- and freeze dried. The solid recovered was calcined at 450 °C under flowing N_2 to bring about cross-linking.

SANS measurements were carried out on V4 instrument at BENSC, Hahn-Meitner Institut, Berlin. A neutron wavelength of 0.457 nm and three sample-detector distances were used (1, 4 and 16 m) in order to cover a Q-range between 4.77 and 6.83 nm^{-1}. Scattering curves obtained from (i) EFW, B4, Al-EFW, Al-B4, MgAl-EFW and FA-B4 dry samples, (ii) Al-EFW and MgAl-EFW samples soaked in two different H_2O–D_2O mixtures, which contrast match either the clay layers or the pillars. The raw data were further corrected for background and empty cell scattering and converted to cross section units after calibration with water by using the BerSANS software developed at BENSC.[8]

The left part of the figure shows the SANS spectra from dry and contrast matched pillared Al-EFW and MgAl-EFW samples. Within the region of high Q values, the characteristic feature for all the pillared samples is the appearance of well-resolved peaks centred at approximately the same Q position and corresponding to real space lengths between 1.40–1.80 nm (Table 1).

Further, when the clay aluminosilicate layers are matched structural information of the pillars is obtained (p samples), revealing that the peaks are still present in both pillared samples that of the MgAl-EFW being more pronounced (inset Fig. 1 left). However, on contrast matching the pillars (samples c) the peaks completely vanish suggesting that the corresponding spacing is characteristic of the distance between pillars. XRD analysis of EFW itself reveals a (001) reflection corresponding to a basal spacing of 1.27 nm, characteristic of the distance

Table 1 Peak position, real space length and surface fractal dimensions

Sample	Q_{peak} (1/nm)	w (nm)	D_s
EFW	—	—	2.60
Al-EFW	3.59	1.75	2.98
MA-EFW	3.57	1.76	2.99
Al-EFW_p	Weak	—	2.93
MA-EFW_p	3.57	1.76	2.98
Al-EFW_c	—	—	2.53
MA-EFW_c	—	—	2.56
B4	—	—	2.60
Al-B4	4.37	1.44	2.74
FA-B4	3.50	1.80	3.09
	4.22	1.49	

DOI: 10.1039/b207392g

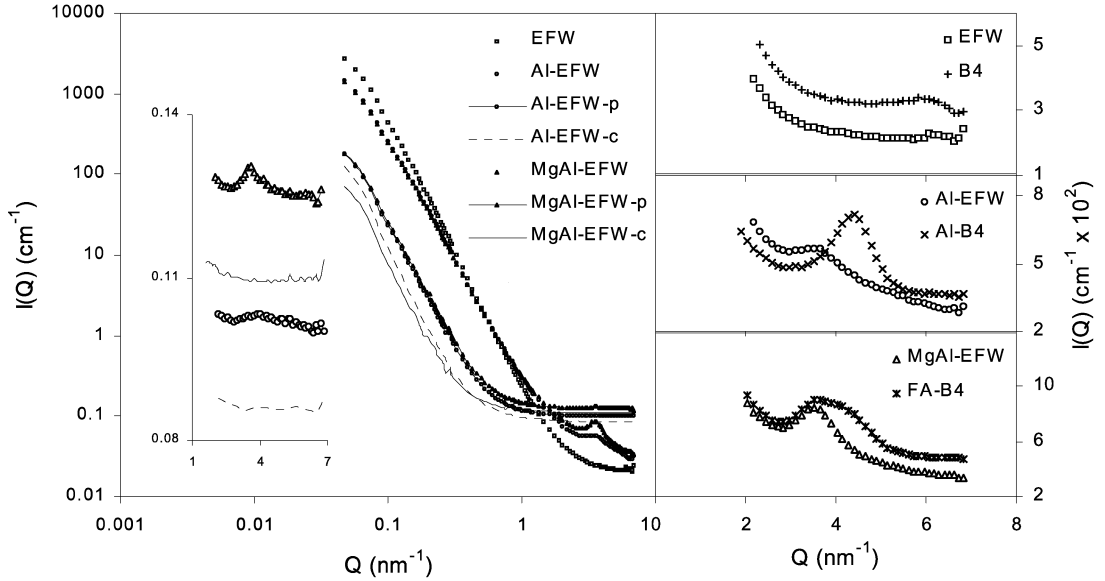

Fig. 1 Left: SANS spectra of parent and pillared EFW clays showing contrast-matching results (inset: high-Q region spectral details of the contrast-matched samples). Right: expanded scale of spectra at Q = 2.0–6.8 nm^{-1} region showing differences between EFWs and B4s.

between lamellae which further increases to 1.73 nm for Al-EFW[9] and 1.87 nm in MgAl-EFW respectively.

The fact that the SANS spectrum from the unpillared sample does not exhibit any peak and the real space distances of the pillared samples are nearly the same, provide additional evidence that the location of the SANS peaks are related to the inter-pillar distance. Also of interest is the increase in scattering in the region of the peak vicinity from the MgAl-EFW sample compared to that in Al-EFW. This can be ascribed to enhanced contrast due to the presence of Mg. In addition, a small decrease of half width in the case of the MgAl-EFW sample may be associated with an increase of the pillar structure orientation (*i.e.* in lateral ordering). Fitting the peak curves leads to an inter-pillar distance of 1.75 nm for Al-EFW and the virtually identical distance of 1.76 nm after Mg^{2+} substitution into the alumina pillar (which confirms that the Mg^{2+} ions are indeed in the pillar). The same analysis for the beidellite series leads to the inter-pillar distances listed in Table 1 derived from Fig. 1 (right). Two facts are obvious: (i) derived w differ greatly from those of the montmorillonite PILCs and (ii) for FA-B4 there are two distinct inter-pillar distances, w_1 = 1.49 nm, and w_2 = 1.80 nm. These are ascribed to differences in ordering provoked by formation of differing chemical bonds between pillars and sheet on calcination. Since basal ordering is the same in both (*i.e.* both possess tetrahedral Si substitution characteristic of beidellites) we conclude that the distances w = 1.44 nm in Al-B4 and w_1 = 1.49 nm and w_2 = 1.80 nm in FA-B4 represent respectively Al–O–Al and Al–(Fe)–O–Si chemical bonds to the clay sheets.

Finally, the surface fractal dimension, D_s can be determined from log $I(Q)$ *vs.* Q plots and are also listed in Table 1. According to the theory, for a smooth surface, D_s = 2, whereas EFW gives D_s = 2.6, suggesting a rather rough and uneven surface, which is further enhanced by pillaring ($D_s \sim 3$ for Al-EFW and MgAl-EFW, respectively). Szücs *et al*. have also observed an uneven surface in a Ca-bentonite sample; the roughness was further increased by Al_2O_3 pillaring and the introduction of Pd nanoparticles.[10] The fact that when the pillared samples here are contrast matched with the clay layers, the fractal dimension remains almost the same ($D_s \sim 3$), confirms that this enhanced surface roughness is due to the effect of pillaring. In addition the pillared contrast matched sample gives back the original clay fractal dimension (D_s = 2.5–2.6). Similar behaviour is observed for the B4 samples.

In conclusion, the contrast-matching SANS technique can be successfully used to determine inter-pillar distances in PILCs; full analysis and its implications for sorption and catalysis is under way.

We gratefully acknowledge the support and encouragement by BENSC, Hahn-Meitner Institute, Berlin, Germany and by the EC (contract HPRI-CT-1999-00020).

Notes and references

1 *Expanded Clays and Other Microporous Materials*, ed. M. Occelli and H. E. Robson, Van Nostrand, New York, 1992; T. J. Pinnavaia and M. F. Thorpe, *Access in Nanoporous Materials*, Plenum, New York and London, 1995.
2 A. A. G. Tomlinson, *J. Porous Mater.*, 1998, **5**, 259.
3 S. Vercauteren, J. Luyten, R. Leysen and E. F. Vansant, *J. Membr. Sci.*, 1996, **119**, 161.
4 J. Miehe-Brendle, L. Khouchaf, J. Baron, R. Le Dred and M. H. Tuilier, *Microporous Mater.*, 1997, **11**, 171; E. Montargès, L. J. Michot and P. Ildefonse, *Microporous Mesoporous Mater.*, 1999, **28**, 83.
5 J. D. F. Ramsay, S. W. Swanton and J. Bunce, *J. Chem. Soc., Faraday Trans.*, 1990, **86**, 3919; F. Pignon, A. Magnin, J. M. Piau, B. Cabane, P. Aimar, M. Meireles and P. Lindner, *J. Membr. Sci.*, 2000, **174**, 189.
6 J. D. F. Ramsay and S. Kallus, *J. Non-Cryst. Solids*, 2001; C. I. Merzbacher, J. G. Barker, K. E. Swider, J. V. Ryan, R. A. Bernstein and D. B. Rolison, *J. Non-Cryst. Solids*, 1998, **255**, 234; E. Hoinkis, *Adv. Colloid Interface Sci.*, 1998, **76–77**, 39; J-C. Li, D. K. Ross, L. D. Howe, K. L. Stefanopoulos, J. P. A. Fairclough, R. Heenan and K. Ibel, *Phys. Rev. B*, 1994, **49**, 5911.
7 A. De Stefanis, G. Perez and A. A. G. Tomlinson, *J. Mater. Chem.*, 1994, **4**, 959; A. De Stefanis, M. Dondi, G. Perez and A. A. G. Tomlinson, *Chemosphere*, 2000, **41**, 1161 and refs. therein for more recent work.
8 U. Keiderling, *Physica B*, 1997, **234–236**, 1111.
9 Th. A. Steriotis, A. De Stefanis and A. A. G. Tomlinson, in preparation.
10 A. Szücs, Z. Király, F. Berger and I. Dékány, *Colloids Surf., A*, 1998, **139**, 109.